Cross-phase modulation mediated pulse control with Airy pulses in optical fibers

IOP Publishing Journal of Optics
J. Opt. 19 (2017) 115505 (7pp) https://doi.org/10.1088/2040-8986/aa8fbf

Cross-phase modulation mediated pulse control with Airy pulses in optical fibers

Michael Goutsoulas, Vassilis Paltoglou and Nikolaos K Efremidis

Department of Mathematics and Applied Mathematics, University of Crete, 70013 Heraklion, Crete, Greece

E-mail: nefrem@uoc.gr

Received 5 July 2017, revised 10 September 2017
Accepted for publication 28 September 2017
Published 20 October 2017

Abstract

We show that the velocity and thus the frequency of a signal pulse can be adjusted by the use of a control Airy pulse. In particular, we utilize a nonlinear Airy pulse which, via cross-phase modulation, creates an effective potential for the optical signal. Interestingly, during the interaction, the signal dispersion is suppressed. Importantly, the whole process is controllable and by using Airy pulses with different truncations leads to predetermined values of the frequency shifting. Such a functionality might be useful in wavelength division multiplexing networks.

Keywords: accelerating pulses, nonlinear optics, optical fibers

(Some figures may appear in colour only in the online journal)

1. Introduction

The study of curved and accelerating waves has attracted a lot of attention over the last years. This interest was triggered by the prediction and experimental observation of exponentially truncated curved Airy beams [1, 2]. The highly desirable properties of the Airy wave (diffraction-free, self-healing [3, 4], and accelerating) have been utilized in a variety of applications from particle manipulation [5, 6], filament generation [7, 8] and electric discharges [9], to beam autofocusing [6, 10, 11], micromachining [12], and high resolution imaging [13, 14].

In the temporal domain, accelerating pulses have been observed in the form of spatiotemporal light bullets [15], and utilized for supercontinuum generation in optical fibers [16], for tuning the frequency of a laser pulse via the use of an Airy pulse-seeded soliton self-frequency shift [17], as well as for high-aspect ratio machining of dielectrics [18]. The presence of third-order dispersion can either increase the acceleration of Airy pulses [19] or cause inversion and tight focusing [20]. Causality effects of accelerating pulses have also been discussed [21].

Of main interest, in connection to this work, is the possibility to modify the properties of an optical signal via the action of cross-phase modulation (XPM) of a nonlinear control pulse. The interaction regimes due to XPM of two pulses and their dynamics have been studied in [22]. The utilization of XPM allows for an optical event horizon or the generation of an optical refractive index barrier [23–25]. Different applications of XPM in all-optical devices have been proposed and observed [26–29]. The non-instantaneous Raman nonlinearity can cause acceleration of a soliton that can be utilized to trap an optical pulse [30, 31]. Our proposal relies on the use of a nonlinear Airy pulse. In this respect, analysis of the nonlinear dynamics of Airy pulses [32, 33] and their Painléve II generalizations [34, 35] have been examined in the literature. Low power Airy pulses have been utilized to achieve control of a solitary wave [36]. In the spatial domain, a two-dimensional Airy beam lattice has been employed to achieve optical routing [37].

In this work, we show that an Airy (control) pulse can be utilized to modify the properties of a Gaussian (signal) pulse. These two pulses have different wavelengths and interact nonlinearly through XPM. In particular, the Airy pulse is nonlinear and through XPM generates an effective potential for the signal. Due to their interaction, the signal pulse (which is linear or moderately nonlinear) is trapped by the effective potential and thus follows the same (temporally translated) accelerating parabolic trajectory. After the interaction, the group velocity and thus the spectrum of the signal pulse are shifted. More importantly, this process is dynamic, and thus by using Airy pulses with different truncations leads to different predetermined values for the spectral shift. Such a functionality might be useful for routing pulses between

different channels in wavelength division multiplexing (WDM) networks. In addition, during the interaction and due to the guiding from the control pulse, the dispersion of the signal is significantly suppressed.

2. Modeling of the system

We start our analysis by considering two pulses of different colors propagating in an optical fiber. Their dynamics can be modeled by the following coupled nonlinear Schrödinger equations

$$\mathrm{i}\left(\frac{\partial A_1}{\partial Z}+\frac{1}{v_{g1}}\frac{\partial A_1}{\partial T}\right)-\frac{\beta_{21}}{2}\frac{\partial^2 A_1}{\partial T^2}+\gamma_1(|A_1|^2+2|A_2|^2)A_1 = \mathrm{i}\frac{\beta_{31}}{6}\frac{\partial^3 A_1}{\partial t^3}+T_{\mathrm{R}}\frac{\partial |A_1|^2}{\partial t}A_1,$$

$$\mathrm{i}\left(\frac{\partial A_2}{\partial Z}+\frac{1}{v_{g2}}\frac{\partial A_2}{\partial T}\right)-\frac{\beta_{22}}{2}\frac{\partial^2 A_2}{\partial T^2}+\gamma_2(|A_2|^2+2|A_1|^2)A_2 = \mathrm{i}\frac{\beta_{32}}{6}\frac{\partial^3 A_2}{\partial t^3}+T_{\mathrm{R}}\frac{\partial |A_2|^2}{\partial t}A_2,$$

where A_1, A_2 are the amplitudes of the electromagnetic field, Z and T are the spatial and temporal coordinates, v_{gj} are the group velocities, β_{2j}, β_{3j}, are the second and third order dispersion coefficients, $\gamma_j = n_2\omega_j/(cA_{\mathrm{eff}})$ are the Kerr nonlinear coefficients ($j = 1, 2$) with A_{eff} being the effective mode area, n_2 is the nonlinear index parameter, ω_j is the respective optical frequency, and c the speed of light. Finally, T_{R} is the coefficient of the Raman nonlinearity. Since the absolute value of the difference between the two frequencies is relatively small $|\omega_1 - \omega_2| \ll \omega_1, \omega_2$ we can approximate $\gamma_1 \approx \gamma_2 \approx \gamma$. The above system of equations can be written in a normalized dimensionless form as

$$\mathrm{i}\frac{\partial u}{\partial z}-\frac{\beta_u}{2}\frac{\partial^2 u}{\partial t^2}+(|u|^2+2|v|^2)u = \mathrm{i}\Delta_u\frac{\partial^3 u}{\partial t^3}+\tau_{\mathrm{R}}\frac{\partial |u|^2}{\partial t}u, \tag{1}$$

$$\mathrm{i}\left(\frac{\partial v}{\partial z}+\alpha\frac{\partial v}{\partial t}\right)-\frac{\beta_v}{2}\frac{\partial^2 v}{\partial t^2}+(|v|^2+2|u|^2)v = \mathrm{i}\Delta_v\frac{\partial^3 v}{\partial t^3}+\tau_{\mathrm{R}}\frac{\partial |v|^2}{\partial t}v. \tag{2}$$

where $\{u, v\} = \sqrt{P_0}\{A_1, A_2\}$ are the field amplitudes, P_0 is a scaling in the power, $z = Z/Z_0$ the spatial and $t = (T - Z/v_{g1})/T_0$ the temporal (retarded) coordinate with $\beta_u = Z_0\beta_{21}/T_0^2$, and $\alpha = Z_0(v_{g1} - v_{g2})/(T_0 v_{g1} v_{g2})$. By defining the dispersion lengths $L_{D,1} = T_0^2/|\beta_{21}|$, $L_{D,2} = T_0^2/|\beta_{22}|$, and the nonlinear length $L_{\mathrm{NL}} = Z_0 = 1/(\gamma P_0)$ we obtain

$$\beta_u = \frac{\mathrm{sgn}\,(\beta_{21})L_{\mathrm{NL}}}{L_{D,1}}, \quad \beta_v = \frac{\mathrm{sgn}\,(\beta_{22})L_{\mathrm{NL}}}{L_{D,2}},$$

$\alpha = z_0(v_{g1} - v_{g2})/(T_0 v_{g1} v_{g2})$, $\tau_{\mathrm{R}} = T_{\mathrm{R}}/T_0$, $\delta_u = \beta_{31}/(6|\beta_{21}|T_0)$, $\delta_v = \beta_{32}/(6|\beta_{22}|T_0)$, $\Delta_u = |\beta_u|\delta_u$, and $\Delta_v = |\beta_v|\delta_v$. Here, we restrict ourselves to group velocity matching conditions and set $\alpha = 0$.

Since minor differences in the profile are not important we choose a Gaussian signal pulse

$$v = F_s \exp[-(t - t_0)^2/\gamma_s^2],$$

where γ_s is the pulse width, F_s is its maximum amplitude, and t_0 is a temporal translation of the pulse with respect to the control pulse. In addition, the control pulse is

$$u = F_c' \mathrm{Ai}\,(\gamma_c t)\exp(\alpha_c t),$$

where α_c is an exponential apodization to make its energy finite (and also determines the total extend of the Airy pulse), γ_c characterizes the width of the main lobe of the pulse, and F_c' is its amplitude. Note that since the maximum value of the Airy function is $\sigma \approx 0.535\,656$, we define $F_c' = F_c/\sigma$, where F_c is the actual maximum amplitude of the control pulse. The Airy pulse, even in the moderately strong nonlinear regime, follows the parabolic trajectory $t = \beta_u^2\gamma_c^3 z^2/4$ (see [1]) and decelerates at is propagates with $v_g = 2/(\beta_u^2\gamma_c^3 z)$. On the other hand, Airy pulses of the form $\mathrm{Ai}\,(-\gamma_c t)$ accelerate during propagation. More importantly there is direct mapping between these two regimes and thus is redundant to study both of these cases separately. For this reason in the rest of the paper we restrict ourselves to the case of decelerating Airy pulses. The generation of an exponentially truncated Airy pulse is possible due to the fact that its Fourier transform is a Gaussian with a cubic phase [1]. The experimental procedure relies on the decomposition of the pulse spectrum by using a grating. Then by applying lenses and a cubic phase mask the Airy pulse can be generated in the Fourier space [15, 38].

We can identify four different regimes in the dynamics associated with the combinations in the signs of the dispersion coefficients (β_u, β_v). An additional parameter is the peak power of the two pulses. Obviously, the control pulse needs to be nonlinear in order to have a measurable effect in the dynamics of the signal pulse via the action of XPM. Furthermore, we select the signal pulse to be linear or weakly nonlinear. If the signal is linear its dynamics do not affect the behavior of the control pulse. However, as we will see, even if the signal pulse is in the moderately nonlinear regime, its dynamics do not significantly effect the Airy pulse due to its self-healing properties.

Since the Airy pulse needs to have relatively strong nonlinearity, the selection of the sign of β_u can significantly affect its dynamics. As it is known [32] in the region of anomalous dispersion accelerating Airy pulses can suffer from soliton shedding. The main problem in this case is that the resulting maximum power of the soliton can be larger than the maximum power of the main Airy lobe and thus (the soliton) significantly interferes in the dynamics. Specifically, if the signal lies in the region of anomalous dispersion, it can get trapped by the potential created by the soliton rather than by the Airy pulse. On the other hand, if the signal lies in the region of normal dispersion the potential barrier created by the soliton can destabilize the dynamics of the signal pulse. Thus, in the present work, we restrict ourselves to the optimal case of Airy pulses propagating in the region of normal dispersion.

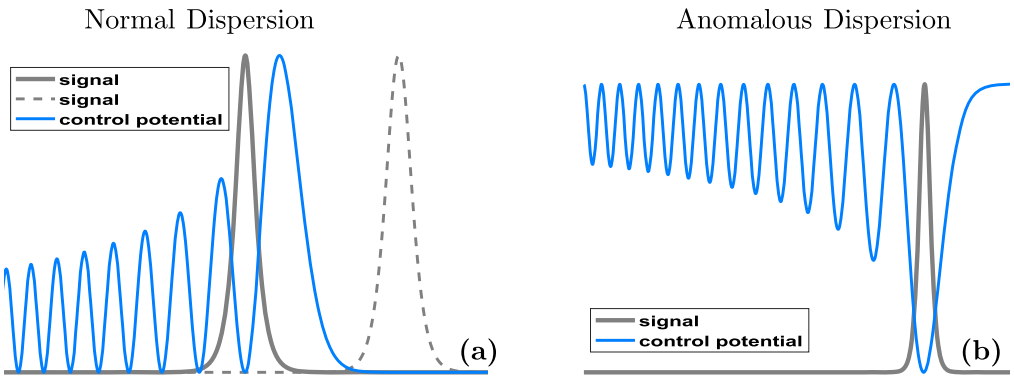

Figure 1. The Airy pulse creates an effective potential (solid blue curve) for the signal pulse (gray solid and dashed–dotted curves). (a) If the signal propagates in the region of normal dispersion then the effective potential is proportional to the power of the Airy pulse. Thus the signal can be either 'dragged' (solid gray curve) or 'pushed' (dashed dotted gray curve) by the potential. (b) If the signal propagates in the region of anomalous dispersion then the effective potential is inversely proportional to the power of the Airy pulse and the signal can be 'dragged' when it is located at potential mimima.

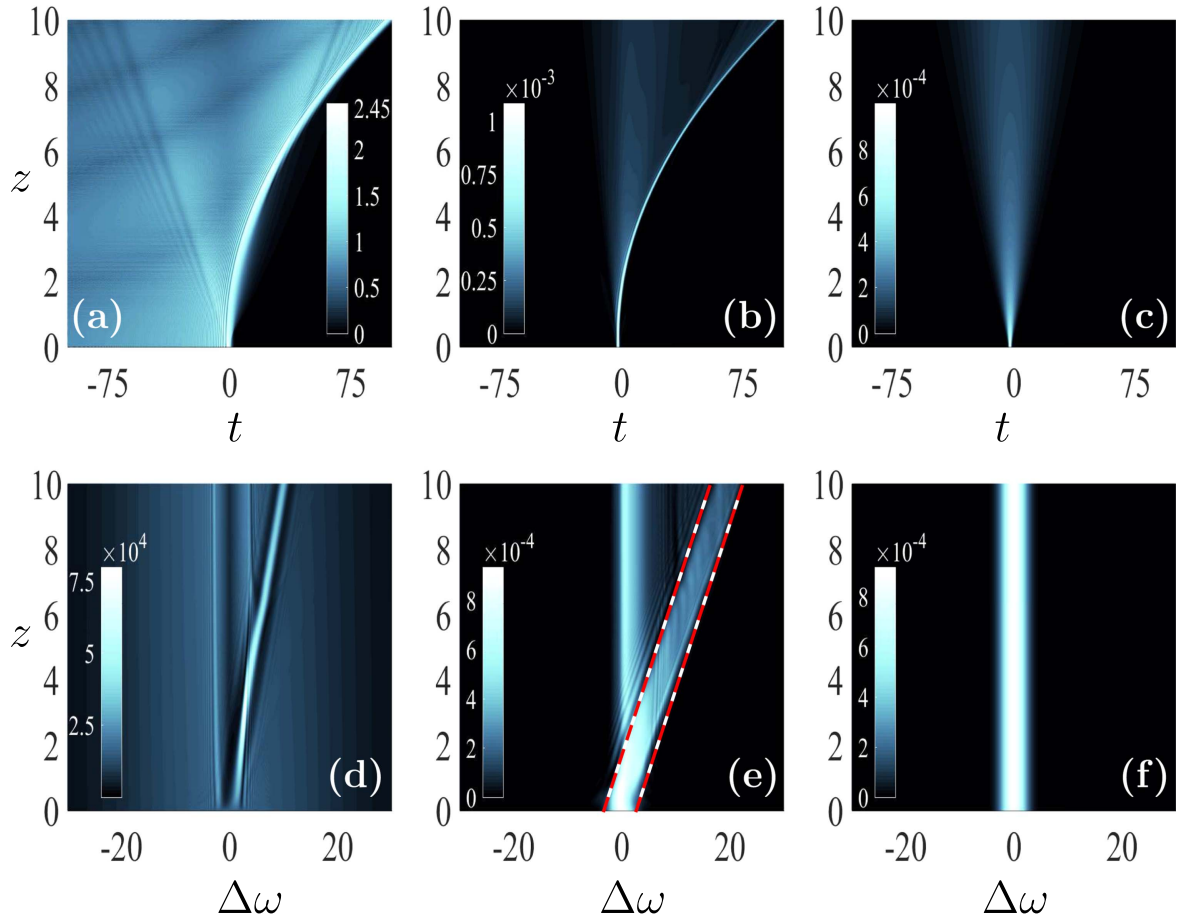

Figure 2. Dynamics of the pulse amplitude (first row) and the corresponding power spectrum (second row) for $\beta_u = 2$, $\beta_v = 1$, $\tau_R = 3/2000$, and $\Delta_u = \Delta_v = 1/1200$. The first two columns depict the control Airy ($|u|$) and the Gaussian signal ($|v|$) pulses, whereas in the third column the dynamics of the signal pulse $|v|$ for $u = 0$ is shown. The signal pulse is effectively linear with $F_s = 0.001$ $\gamma_s = 0.651$ and $t_0 = -2.3482$ (positioned between main and secondary lobe), while for the control pulse $F_c = 2.5$, $\gamma_c = 1$, and $\alpha_c = 0.001$.

The sign of the dispersion β_v is also significant because it determines the kind of potential that the signal it is subjected to. Let us denote as the first minimum (or maximum) of the Airy function the rightmost one and then continue counting along the negative axis. In the same fashion we can enumerate the local maxima of the Airy function (the first one being the global maximum). As can be seen in figure 1 the Airy pulse, due to XPM, creates an effective potential for the signal. In the region of normal dispersion, this potential is proportional to the power of the Airy pulse and, thus, the signal can be

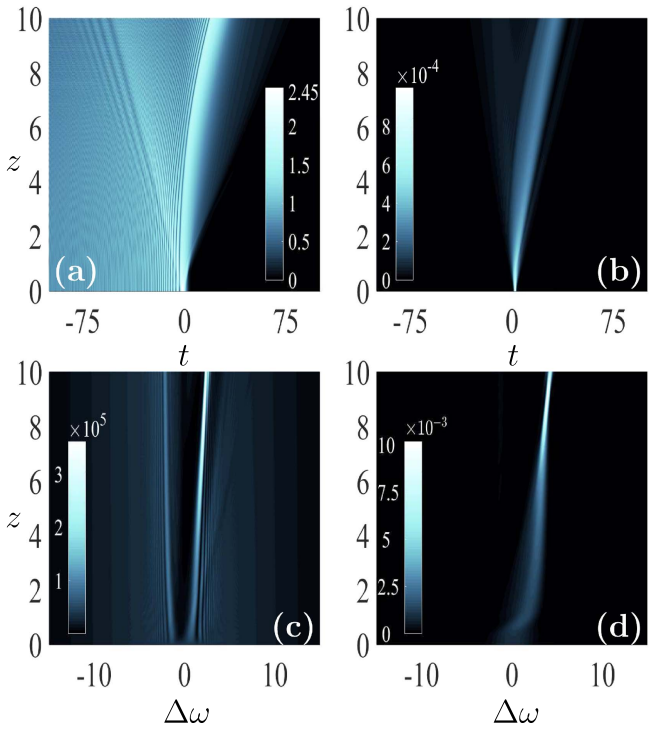

Figure 3. Dynamics of the control and the signal pulse (first row) and the corresponding spectra (second row) when the signal is launched after the Airy pulse ($t_0 = 2.3482$) for $\beta_u = 2$, $\beta_v = 1$, $\tau_R = 3/2000$, and $\Delta_u = \Delta_v = 1/1200$. The signal pulse propagates under essentially linear conditions with $F_s = 0.001$, $\gamma_s = 0.651$, and $t_0 = 2.3482$, while for the control pulse $F_c = 2.5$, $\gamma_c = 0.65$, and $\alpha_c = 0.001$.

trapped if it is located in an Airy minimum. Furthermore, as the control pulse is accelerating, we expect the signal to follow the same kind of trajectory. We call this behavior 'dragging'. As we shift to higher numbers of minima the potential barrier contrast is decreased. In addition, the frequency of the oscillations increases making the barrier 'thinner'. In this respect, the first minima are preferable. In addition, the signal pulse can be located to the right of the Airy pulse. Thus, as the Airy pulse accelerates, it can 'push' the signal pulse (figure 1(a) dashed line). On the other hand, if the signal propagates in the region of anomalous dispersion, the effective potential created by the Airy pulse is inversely proportional to its power. Thus, in order to facilitate the dragging behavior, the signal pulse should be located to a maximum of the Airy function. The first lobe creates the strongest potential well, and thus is preferable. However, even subsequent lobes of the Airy pulse can be utilized to drag the optical signal.

3. Numerical results

All our simulations were carried out by utilizing a 4th order split-step Fourier scheme [39]. In addition, we select typical values for $\beta_{3j} = 0.1$ ps^3 km^{-1}, $T_R = 3$ fs, $|\beta_{21}| = 20$ ps^2 km^{-1}, and $T_0 = 2$ ps. The dispersion of the signal pulse is then obtained though $\beta_{22} = \beta_v\beta_{21}/\beta_u$. Note that in all of the cases studied below, the Airy pulse propagates in the region of normal dispersion, and the effect of higher order terms (Raman nonlinearity and third order dispersion) is insignificant. By comparing the simulation results produced with and without these terms, we see that they are nearly identical. This can be explained by the fact that in the region of normal dispersion the main lobe of the Airy pulse has the tendency to effectively 'defocus'. In addition, following a ray optics approach, the rays that contribute to the generation of the Airy pulse originate from the low intensity tails of the Airy pulse and are different at each propagation distance. On the other hand, in the case where the Airy pulse propagates in the anomalous dispersion regime (which is not examined in this work), we can see the soliton (generated by shedding from the Airy pulse) decelerating due to the Raman effect.

First, we examine the case where both pulses propagate in the normal dispersion regime. In the results shown in figure 2 the signal pulse is linear. Thus, if the control pulse is absent, the signal maintains its spectrum and temporal profile, and disperses as it propagates (figure 2, 3rd column). In the first two columns of figure 2, we see the dynamics when both pulses co-propagate inside the fiber. We note that the spectrum of the Airy pulse changes during propagation due to its nonlinear self-action [33]. This mainly involves frequencies in the central part of the spectrum that are blue-shifted. However, the spectral tails, representing the driving force of the Airy pulse are not affected up to $z = 10$. In figure 2(b), we can see the dynamics of the signal pulse, which is originally positioned between the main and the secondary lobe. Due to the presence of the effective potential from the control, the optical signal is dragged along the parabolic trajectory. We note that as the signal accelerates a part of its energy turns into low amplitude radiation. In addition, the dispersion of the signal is strongly suppressed (compare figures 2(b) and (c))). In figure 2(e) we depict the power spectrum $|\tilde{v}(\omega)|^2$ of the signal pulse. At the initial stages of propagation, we clearly see a splitting in the spectrum: the left branch, associated with the radiation, remains almost invariant during propagation. The part of the spectrum that linearly translates to the right is associated with the accelerating signal. Taking into account the group velocity of the Airy pulse

$$v_g = \frac{2}{\beta_u^2\gamma_c^2 z}$$

which is equalized to the group velocity of the control pulse

$$v_g = \frac{1}{\beta_v\Delta\omega}$$

we obtain the frequency shift of the signal pulse as it propagates through the fiber

$$\Delta\omega = \frac{\beta_u^2\gamma_c^3 z}{2\beta_v}. \quad (3)$$

We see that, as long as the signal is dragged by the control pulse, its frequency is shifting linearly with the propagation distance. The red lines in figure 2(e) are translations of equation (3) to depict the spectral range of the accelerating

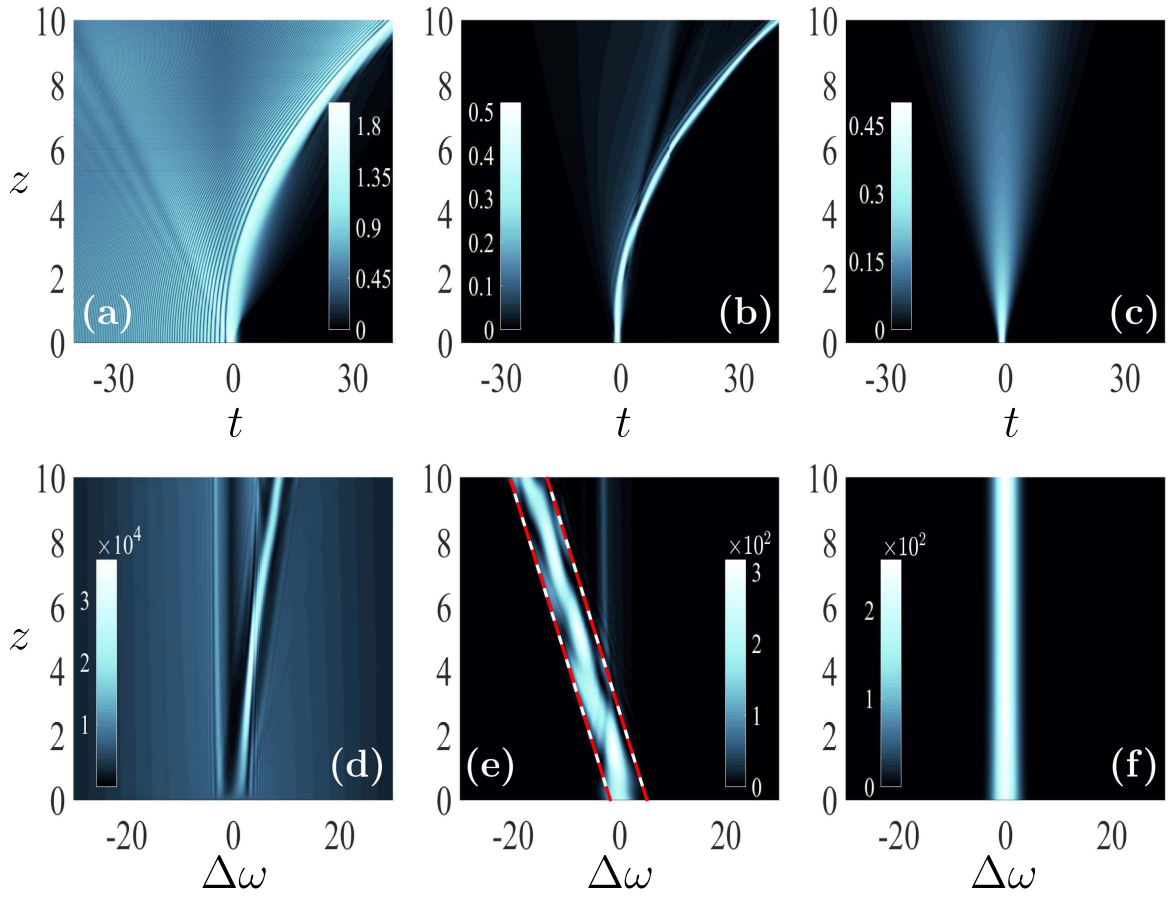

Figure 4. Dynamics of the pulse amplitude (first row) and the corresponding power spectrum (second row) for $F_s = 0.5$, $\gamma_s = 0.651$, $t_0 = -0.8789$ (the signal positioned in the main Airy lobe, see figure 1(b)), $F_c = 2$, $\gamma_c = 1.2$, $\alpha_c = 0.001$, $\beta_u = 1$, $\beta_v = -1/2$, $\tau_R = 3/2000$, and $\Delta_u = \Delta_v = 1/2400$.

signal. Note the excellent agreement between theoretical and numerical results.

In addition to the aforementioned case, the signal pulse can be launched after the Airy pulse (figure 1(a) dashed–dotted curve). Thus, during propagation the signal is 'pushed' from one side from the Airy pulse, but from the other side it can still disperse. In figure 3, we depict the dynamics of the signal and the control pulses in the real and in the Fourier space. As we can see, the signal continues to disperse during acceleration. Perhaps the most interesting feature in the dynamics is that the spectrum of the signal gets significantly compressed as it propagates.

Next, we examine the case where the signal pulse propagates in the anomalous dispersion regime. We select the signal maximum to be positioned at the main lobe of the Airy pulse (figure 1(b)). The power of the signal is relatively strong but not strong enough to generate a soliton, as depicted in figure 4(c) where the dynamics of the signal in the absence of the control is shown. In the first two columns of figure 4, we see the dynamics when both pulses co-propagate inside the fiber. In this case, the signal is nonlinear and thus is expected to, in principle, affect the control via XPM. However, since the nonlinearity of the signal is not very strong we do not observe any significant signs of this interaction in the control pulse. This is demonstrated in figure 5 where the parameters are the same, except that the signal is linear.

The potential to shift the frequency of a signal pulse might be used in optical networks to achieve, for example, all-optical switching between different WDM channels. In order to do so, we use Airy pulses that are truncated (their amplitude becomes zero) after a specific numbers of lobes. The larger the number of lobes of the control pulse, the longer the interaction between the two pulses is going to last, leading to a bigger value in the frequency shift of the signal. The number of lobes of the Airy pulse can be designed so that, after the interaction takes place, the signal pulses are switched to specific channels of a WDM network. An example is shown in figure 5, where Airy pulses with 10, 30, and 70 lobes are selected. We clearly see that after the interaction with the control pulse, and depending on the number of lobes, the signal is associated with a different group velocity and thus with a different frequency.

4. Conclusions

In conclusion, we have shown that the frequency and thus the velocity of a signal pulse can be shifted by the use of an Airy pulse via XPM. More importantly, the whole process is

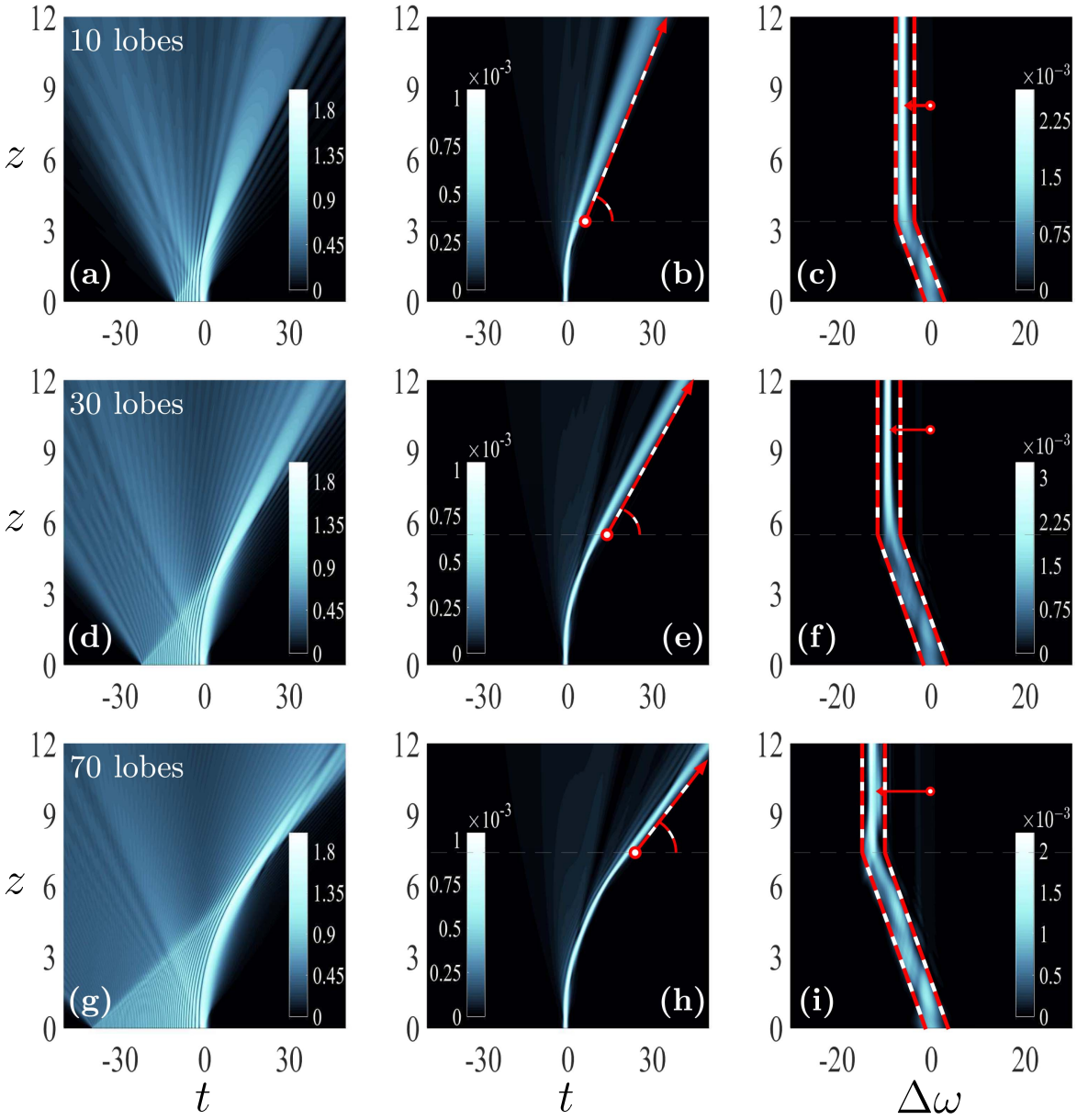

Figure 5. In the three rows the interaction dynamics of an Airy pulse with 10, 30, and 70 lobes with a Gaussian signal is depicted. The three columns show the amplitude of the Airy pulse $|u|$, the signal pulse $|v|$ and its power spectrum $|\tilde{v}|^2$. The signal is essentially linear and $\gamma_s = 0.651$, $F_s = 0.001$, $t_0 = -0.8789$ while for the control pulse $F_c = 2$, $\gamma_c = 1.2$ and $\alpha_c = 0.001$. The parameters are $\beta_u = 1$, $\beta_v = -1/2$, $\tau_R = 3/2000$, and $\Delta_u = \Delta_v = 1/2400$.

controllable and by using Airy pulses with different truncations can lead to predetermined values of the signal frequency shift. Such a functionality might be useful in WDM networks.

Acknowledgments

MG is supported from the Greek State Scholarships Foundation (IKY). NKE is supported by the Erasmus Mundus NANOPHI Project (contract number 2013-5659/002-001).

ORCID iDs

Nikolaos K Efremidis https://orcid.org/0000-0002-9830-0268

References

[1] Siviloglou G A and Christodoulides D N 2007 Accelerating finite energy Airy beams *Opt. Lett.* **32** 979–81
[2] Siviloglou G A, Broky J, Dogariu A and Christodoulides D N 2007 Observation of accelerating Airy beams *Phys. Rev. Lett.* **99** 213901

[3] Broky J, Siviloglou G A, Dogariu A and Christodoulides D N 2008 Self-healing properties of optical Airy beams *Opt. Express* **16** 12880–91
[4] Hu Y, Zhang P, Lou C, Huang S, Xu J and Chen Z 2010 Optimal control of the ballistic motion of Airy beams *Opt. Lett.* **35** 2260–2
[5] Baumgartl J, Mazilu M and Dholakia K 2008 Optically mediated particle clearing using Airy wavepackets *Nat. Photon.* **2** 675–8
[6] Zhang P, Prakash J, Zhang Z, Mills M S, Efremidis N K, Christodoulides D N and Chen Z 2011 Trapping and guiding microparticles with morphing autofocusing Airy beams *Opt. Lett.* **36** 2883–5
[7] Polynkin P, Kolesik M, Moloney J V, Siviloglou G A and Christodoulides D N 2009 Curved plasma channel generation using ultraintense Airy beams *Science* **324** 229–32
[8] Polynkin P, Kolesik M and Moloney J 2009 Filamentation of femtosecond laser Airy beams in water *Phys. Rev. Lett.* **103** 123902
[9] Clerici M *et al* 2015 Laser-assisted guiding of electric discharges around objects *Sci. Adv.* **1** 1400111
[10] Efremidis N K and Christodoulides D N 2010 Abruptly autofocusing waves *Opt. Lett.* **35** 4045–7
[11] Papazoglou D G, Efremidis N K, Christodoulides D N and Tzortzakis S 2011 Observation of abruptly autofocusing waves *Opt. Lett.* **36** 1842–4
[12] Mathis A, Courvoisier F, Froehly L, Furfaro L, Jacquot M, Lacourt P A and Dudley J M 2012 Micromachining along a curve: femtosecond laser micromachining of curved profiles in diamond and silicon using accelerating beams *Appl. Phys. Lett.* **101** 071110
[13] Jia S, Vaughan J C and Zhuang X 2014 Isotropic three-dimensional super-resolution imaging with a self-bending point spread function *Nat. Photon.* **8** 302–6
[14] Vettenburg T, Dalgarno H I C, Nylk J, Coll-Lladó C, Ferrier D E K, Cizmar T, Gunn-Moore F J and Dholakia K 2014 Light-sheet microscopy using an Airy beam *Nat. Methods* **11** 541–4
[15] Chong A, Renninger W H, Christodoulides D N and Wise F W 2010 Airy–Bessel wave packets as versatile linear light bullets *Nat. Photon.* **4** 103–6
[16] Ament C, Polynkin P and Moloney J V 2011 Supercontinuum generation with femtosecond self-healing Airy pulses *Phys. Rev. Lett.* **107** 243901
[17] Hu Y, Tehranchi A, Wabnitz S, Kashyap R, Chen Z and Morandotti R 2015 Improved intrapulse raman scattering control via asymmetric Airy pulses *Phys. Rev. Lett.* **114** 073901
[18] Götte N, Winkler T, Meinl T, Kusserow T, Zielinski B, Sarpe C, Senftleben A, Hillmer H and Baumert T 2016 Temporal Airy pulses for controlled high aspect ratio nanomachining of dielectrics *Optica* **3** 389–95
[19] Besieris I M and Shaarawi A M 2008 Accelerating Airy wave packets in the presence of quadratic and cubic dispersion *Phys. Rev.* E **78** 046605
[20] Driben R, Hu Y, Chen Z, Malomed B A and Morandotti R 2013 Inversion and tight focusing of Airy pulses under the action of third-order dispersion *Opt. Lett.* **38** 2499–501
[21] Kaminer I, Lumer Y, Segev M and Christodoulides D N 2011 Causality effects on accelerating light pulses *Opt. Express* **19** 23132–9
[22] Agrawal G P, Baldeck P L and Alfano R R 1989 Temporal and spectral effects of cross-phase modulation on copropagating ultrashort pulses in optical fibers *Phys. Rev.* A **40** 5063–72
[23] Philbin T G, Kuklewicz C, Robertson S, Hill S, König F and Leonhardt U 2008 Fiber-optical analog of the event horizon *Science* **319** 1367–70
[24] Skryabin D V and Yulin A V 2005 Theory of generation of new frequencies by mixing of solitons and dispersive waves in optical fibers *Phys. Rev.* E **72** 016619
[25] Webb K E, Erkintalo M, Xu Y, Broderick N G, Dudley J M, Genty G and Murdoch S G 2013 Nonlinear optics of fibre event horizons *Nat. Commun.* **5** 4969–4969
[26] Sharping J E, Fiorentino M, Kumar P and Windeler R S 2002 All-optical switching based on cross-phase modulation in microstructure fiber *IEEE Photon. Technol. Lett.* **14** 77–9
[27] Mizrahi V, Larochelle S, Hibino Y and Stegeman G I 1990 All-optical switching of grating transmission using cross-phase modulation in optical fibres *Electron. Lett.* **26** 1459–60
[28] Bogris A, Velanas P and Syvridis D 2007 Numerical investigation of a 160-gb/s reconfigurable photonic logic gate based on cross-phase modulation in fibers *IEEE Photon. Technol. Lett.* **19** 402–4
[29] Qiu J, Sun K, Rochette M and Chen L R 2010 Reconfigurable all-optical multilogic gate (XOR, AND, and OR) based on cross-phase modulation in a highly nonlinear fiber *IEEE Photon. Technol. Lett.* **22** 1199–201
[30] Gorbach A V and Skryabin D V 2007 Theory of radiation trapping by the accelerating solitons in optical fibers *Phys. Rev.* A **76** 053803
[31] Nishizawa N and Goto T 2002 Pulse trapping by ultrashort soliton pulses in optical fibers across zero-dispersion wavelength *Opt. Lett.* **27** 152–4
[32] Fattal Y, Rudnick A and Marom D M 2011 Soliton shedding from Airy pulses in kerr media *Opt. Express* **19** 17298–307
[33] Hu Y, Li M, Bongiovanni D, Clerici M, Yao J, Chen Z, Azaña J and Morandotti R 2013 Spectrum to distance mapping via nonlinear Airy pulses *Opt. Lett.* **38** 380–2
[34] Giannini J A and Joseph R I 1989 The role of the second painlevé transcendent in nonlinear optics *Phys. Lett.* A **141** 417–9
[35] Kaminer I, Segev M and Christodoulides D N 2011 Self-accelerating self-trapped optical beams *Phys. Rev. Lett.* **106** 213903
[36] Cai W, Mills M S, Christodoulides D N and Wen S 2014 Soliton manipulation using Airy pulses *Opt. Commun.* **316** 127–31
[37] Rose P, Diebel F, Boguslawski M and Denz C 2013 Airy beam induced optical routing *Appl. Phys. Lett.* **102** 101101
[38] Weiner A M 2000 Femtosecond pulse shaping using spatial light modulators *Rev. Sci. Instrum.* **71** 1929–60
[39] Agrawal G 2013 *Nonlinear Fiber Optics* 5th edn (Boston, MA: Academic)